

Outage Probability of the Gaussian MIMO Free-Space Optical Channel with PPM

Nick Letzepis, *Member, IEEE* and Albert Guillén i Fàbregas, *Member, IEEE*

Abstract

The free-space optical channel has the potential to facilitate inexpensive, wireless communication with fiber-like bandwidth under short deployment timelines. However, atmospheric effects can significantly degrade the reliability of a free-space optical link. In particular, atmospheric turbulence causes random fluctuations in the irradiance of the received laser beam, commonly referred to as *scintillation*. The scintillation process is slow compared to the large data rates typical of optical transmission. As such, we adopt a quasi-static block fading model and study the outage probability of the channel under the assumption of orthogonal pulse-position modulation. We investigate the mitigation of scintillation through the use of multiple lasers and multiple apertures, thereby creating a multiple-input multiple output (MIMO) channel. Non-ideal photodetection is also assumed such that the combined shot noise and thermal noise are considered as signal-independent additive Gaussian white noise. Assuming perfect receiver channel state information (CSI), we compute the signal-to-noise ratio exponents for the cases when the scintillation is lognormal, exponential and gamma-gamma distributed, which cover a wide range of atmospheric turbulence conditions. Furthermore, we illustrate very large gains, in some cases larger than 15 dB, when transmitter CSI is also available by adapting the transmitted electrical power.

I. INTRODUCTION

Free-space optical (FSO) communication offers an attractive alternative to the radio frequency (RF) channel for the purpose of transmitting data at very high rates. By utilising a high carrier frequency in the optical range, digital communication on the order of gigabits per second is

N. Letzepis is with Institute for Telecommunications Research, University of South Australia, SPRI Building - Mawson Lakes Blvd., Mawson Lakes SA 5095, Australia, e-mail: nick.letzepis@unisa.edu.au.

A. Guillén i Fàbregas is with the Department of Engineering, University of Cambridge, Cambridge CB2 1PZ, UK, e-mail: guillen@ieee.org.

possible. In addition, FSO links are difficult to intercept, immune to interference or jamming from external sources, and are not subject to frequency spectrum regulations. FSO communications have received recent attention in applications such as satellite communications, fiber-backup, RF-wireless back-haul and last-mile connectivity [1].

The main drawback of the FSO channel is the detrimental effect the atmosphere has on a propagating laser beam. The atmosphere is composed of gas molecules, water vapor, pollutants, dust, and other chemical particulates that are trapped by Earth's gravitational field. Since the wavelength of a typical optical carrier is comparable to these molecule and particle sizes, the carrier wave is subject to various propagation effects that are uncommon to RF systems. One such effect is *scintillation*, caused by atmospheric turbulence, and refers to random fluctuations in the irradiance of the received optical laser beam (analogous to fading in RF systems) [2–4].

Recent works on the mitigation of scintillation concentrate on the use of multiple-lasers and multiple-apertures to create a multiple-input-multiple-output (MIMO) channel [5–13]. Many of these works consider scintillation as an ergodic fading process, and analyse the channel in terms of its ergodic capacity. However, compared to typical data rates, scintillation is a slow time-varying process (with a coherence time on the order of milliseconds), and it is therefore more appropriate to analyse the outage probability of the channel. To some extent, this has been done in the works of [6, 10, 12–14]. In [6, 13] the outage probability of the MIMO FSO channel is analysed under the assumption of ideal photodetection (i.e. a Poisson counting process) with no bandwidth constraints. Wilson *et al.* [10] also assume perfect photodetection, but with the further constraint of pulse-position modulation (PPM). Lee and Chan [12], study the outage probability under the assumption of on-off keying (OOK) transmission and non-ideal photodetection, i.e. the combined shot noise and thermal noise process is modeled as zero mean signal independent additive white Gaussian noise (AWGN). Farid and Hranilovic [14] extend this analysis to include the effects of pointing errors.

In this paper we study the outage probability of the MIMO FSO channel under the assumptions of PPM, non-ideal photodetection, and equal gain combining (EGC) at the receiver. In particular, we model the channel as a quasi-static block fading channel whereby communication takes place over a finite number of blocks and each block of transmitted symbols experiences an independent identically distributed (i.i.d.) fading realisation [15, 16]. We consider two types of CSI knowledge. First we assume perfect CSI is available only at the receiver (CSIR case), and the

transmitter knows only the channel statistics. Then we consider the case when perfect CSI is also known at the transmitter (CSIT case).¹ Under this framework we study a number of scintillation distributions: lognormal, modelling weak turbulence; exponential, modelling strong turbulence; and gamma-gamma [17], which models a wide range of turbulence conditions. For the CSIR case, we derive signal-to-noise ratio (SNR) exponents and show that they are the product of: a channel related parameter, dependent on the scintillation distribution; the number of lasers times the number of apertures, reflecting the spatial diversity; and the Singleton bound [18–20], reflecting the block diversity. For the CSIT case, the transmitter finds the optimal power allocation that minimises the outage probability [21]. Using results from [22], we derive the optimal power allocation subject to short- and long-term power constraints. We show that very large power savings are possible compared to the CSIR case. Interestingly, under a long-term power constraint, we show that delay-limited capacity [23] is zero for exponential and (in some cases) gamma-gamma scintillation, unless one codes over multiple blocks, and/or uses multiple lasers and apertures.

The paper is organised as follows. In Section II, we define the channel model and assumptions. In Section III we review the lognormal, exponential and gamma-gamma models. Section IV defines the outage probability and presents results on the minimum-mean squared error (MMSE). Then in Sections V and VI we present the main results of our asymptotic outage probability analysis for the CSIR and CSIT cases, respectively. Concluding remarks are then given in Section VII. Proofs of the various results can be found in the Appendices.

II. SYSTEM MODEL

We consider an $M \times N$ MIMO FSO system with M transmit lasers and N aperture receiver as shown in Fig. 1. Information data is first encoded by a binary code of rate R_c . The encoded stream is modulated according to a Q -ary PPM scheme, resulting in rate $R = R_c \log_2 Q$ (bits/channel use). Repetition transmission is employed such that the same PPM signal is transmitted in perfect synchronism by each of the M lasers through an atmospheric turbulent channel and collected by N receive apertures. We assume the distance between the individual lasers and apertures is

¹Given the slow time-varying scintillation process, CSI can be estimated at the receiver and fed back to the transmitter via a dedicated feedback link.

sufficient so that spatial correlation is negligible. At each aperture, the received optical signal is converted to an electrical signal via photodetection. Non-ideal photodetection is assumed such that the combined shot noise and thermal noise processes can be modeled as zero mean, signal independent AWGN (an assumption commonly used in the literature, see e.g. [3–5, 12, 14, 24–29]).

In FSO communications, channel variations are typically much slower than the signaling period. As such, we model the channel as a non-ergodic block-fading channel, for which a given codeword of length BL undergoes only a finite number B of scintillation realisations [15, 16]. The received signal at aperture n , $n = 1, \dots, N$ can be written as

$$\mathbf{y}_b^n[\ell] = \left(\sum_{m=1}^M \tilde{h}_b^{m,n} \right) \sqrt{\tilde{p}_b} \mathbf{x}_b[\ell] + \tilde{\mathbf{z}}_b^n[\ell], \quad (1)$$

for $b = 1, \dots, B, \ell = 1, \dots, L$, where $\mathbf{y}_b^n[\ell], \tilde{\mathbf{z}}_b^n[\ell] \in \mathbb{R}^Q$ are the received and noise signals at block b , time instant ℓ and aperture n , $\mathbf{x}_b[\ell] \in \mathbb{R}^Q$ is the transmitted signal at block b and time instant ℓ , and $\tilde{h}_b^{m,n}$ denotes the scintillation fading coefficient between laser m and aperture n . Each transmitted symbol is drawn from a PPM alphabet, $\mathbf{x}_b[\ell] \in \mathcal{X}^{\text{ppm}} \triangleq \{\mathbf{e}_1, \dots, \mathbf{e}_Q\}$, where \mathbf{e}_q is the canonical basis vector, i.e., it has all zeros except for a one in position q , the time slot where the pulse is transmitted. The noise samples of $\tilde{\mathbf{z}}_b^n[\ell]$ are independent realisations of a random variable $Z \sim \mathcal{N}(0, 1)$, and \tilde{p}_b denotes the received electrical power of block b at each aperture in the absence of scintillation. The fading coefficients $\tilde{h}_b^{m,n}$ are independent realisations of a random variable \tilde{H} with probability density function (pdf) $f_{\tilde{H}}(h)$.

At the receiver, we assume equal gain combining (EGC) is employed, such that the entire system is equivalent to a single-input single-output (SISO) channel, i.e.

$$\mathbf{y}_b[\ell] = \frac{1}{\sqrt{N}} \sum_{n=1}^N \mathbf{y}_b^n[\ell] = \sqrt{p_b} h_b \mathbf{x}_b[\ell] + \mathbf{z}_b[\ell], \quad (2)$$

where $\mathbf{z}_b[\ell] = \frac{1}{\sqrt{N}} \sum_{n=1}^N \tilde{\mathbf{z}}_b^n[\ell] \sim \mathcal{N}(0, 1)$, and h_b , a realisation of the random variable H , is defined as the normalised combined fading coefficient, i.e.

$$h_b = \frac{c}{MN} \sum_{m=1}^M \sum_{n=1}^N \tilde{h}_b^{m,n}, \quad (3)$$

where $c = 1/(\mathbb{E}[\tilde{H}]\sqrt{1 + \sigma_I^2/(MN)})$ is a constant to ensure $\mathbb{E}[H^2] = 1$.² Thus, the total instantaneous received electrical power at block b is $p_b = M^2 N \tilde{p}_b / c$, and the total average received SNR is $\text{snr} \triangleq \mathbb{E}[h_b p_b] = \mathbb{E}[p_b]$.

For the CSIR case, we assume the electrical power is distributed uniformly over the blocks, i.e., $p_b = p = \text{snr}$ for $b = 1, \dots, B$. Otherwise, for the CSIT case, we will allocate electrical power in order to improve performance. In particular, we will consider the following two electrical power constraints

$$\text{Short-term: } \frac{1}{B} \sum_{b=1}^B p_b \leq P \quad (4)$$

$$\text{Long-term: } \mathbb{E} \left[\frac{1}{B} \sum_{b=1}^B p_b \right] \leq P. \quad (5)$$

Throughout the paper, we will devote special attention to the case of $B = 1$, i.e., the channel does not vary within a codeword. This scenario is relevant for FSO, since, due to the large data-rates, one is able to transmit millions of bits over the same channel realisation. We will see that most results admit very simple forms, and some cases, even closed form. This analysis allows for a system characterisation where the expressions highlight the roles of the key design parameters.

III. SCINTILLATION DISTRIBUTIONS

The scintillation pdf, $f_{\tilde{H}}(h)$, is parameterised by the *scintillation index* (SI),

$$\sigma_I^2 \triangleq \frac{\text{Var}(\tilde{H})}{(\mathbb{E}[\tilde{H}])^2}, \quad (6)$$

and can be considered as a measure of the strength of the optical turbulence under weak turbulence conditions [17, 30].

The distribution of the irradiance fluctuations is dependent on the strength of the optical turbulence. For the weak turbulence regime, the fluctuations are generally considered to be

²For optical channels with ideal photodetection, the normalisation $\mathbb{E}[H] = 1$ is commonly used to keep optical power constant. We assume non-ideal photodetection and work entirely in the electrical domain. Hence, we chose the normalisation $\mathbb{E}[H^2] = 1$, used commonly in RF fading channels. However, since we consider only the asymptotic behaviour of the outage probability, the specific normalisation is irrelevant and does not affect our results.

lognormal distributed, and for very strong turbulence, exponential distributed [2, 31]. For moderate turbulence, the distribution of the fluctuations is not well understood, and a number of distributions have been proposed, such as the lognormal-Rice distribution [4, 17, 32–34] (also known as the Beckmann distribution [35]) and K-distribution [32]. In [17], Al-Habash *et al.* proposed a gamma-gamma distribution as a general model for all levels of atmospheric turbulence. Moreover, recent work in [34] has shown that the gamma-gamma model is in close agreement with experimental measurements under moderate-to-strong turbulence conditions. In this paper we focus on lognormal, exponential, and gamma-gamma distributed scintillation, which are described as follows.

For lognormal distributed scintillation,

$$f_{\tilde{H}}^{\text{ln}}(h) = \frac{1}{h\sigma\sqrt{2\pi}} \exp\left(-(\log h - \mu)^2 / (2\sigma^2)\right), \quad (7)$$

where μ and σ are related to the SI via $\mu = -\log(1 + \sigma_I^2)$ and $\sigma^2 = \log(1 + \sigma_I^2)$.

For exponential distributed scintillation

$$f_{\tilde{H}}^{\text{exp}}(h) = \lambda \exp(-\lambda h) \quad (8)$$

which corresponds to the super-saturated turbulence regime, where $\sigma_I^2 = 1$.

The gamma-gamma distribution arises from the product of two independent Gamma distributed random variables and has the pdf [17],

$$f_{\tilde{H}}^{\text{gg}}(h) = \frac{2(\alpha\beta)^{\frac{\alpha+\beta}{2}}}{\Gamma(\alpha)\Gamma(\beta)} h^{\frac{\alpha+\beta}{2}-1} K_{\alpha-\beta}(2\sqrt{\alpha\beta h}), \quad (9)$$

where $K_\nu(x)$ denotes the modified Bessel function of the second kind [36, Ch. 10]. The parameters α and β are related with the scintillation index via $\sigma_I^2 = \alpha^{-1} + \beta^{-1} + (\alpha\beta)^{-1}$.

IV. INFORMATION THEORETIC PRELIMINARIES

The channel described by (2) under the quasi-static assumption is not information stable [37] and therefore, the channel capacity in the strict Shannon sense is zero. It can be shown that the codeword error probability of any coding scheme is lower bounded by the information outage probability [15, 16],

$$P_{\text{out}}(\text{snr}, R) = \Pr(I(\mathbf{p}, \mathbf{h}) < R), \quad (10)$$

where R is the transmission rate and $I(\mathbf{p}, \mathbf{h})$ is the instantaneous input-output mutual information for a given power allocation $\mathbf{p} \triangleq (p_1, \dots, p_B)$, and vector channel realisation $\mathbf{h} \triangleq (h_1, \dots, h_B)$. The instantaneous mutual information can be expressed as [38]

$$I(\mathbf{p}, \mathbf{h}) = \frac{1}{B} \sum_{b=1}^B I^{\text{awgn}}(p_b h_b^2), \quad (11)$$

where $I^{\text{awgn}}(\rho)$ is the input-output mutual information of an AWGN channel with SNR ρ . For PPM [24]

$$I^{\text{awgn}}(\rho) = \log_2 Q - \mathbb{E} \left[\log_2 \left(1 + \sum_{q=2}^Q e^{-\rho + \sqrt{\rho}(Z_q - Z_1)} \right) \right], \quad (12)$$

where $Z_q \sim \mathcal{N}(0, 1)$ for $q = 1, \dots, Q$.

For the CSIT case we will use the recently discovered relationship between mutual information and the MMSE [39]. This relationship states that³

$$\frac{d}{d\rho} I^{\text{awgn}}(\rho) = \frac{\text{mmse}(\rho)}{\log(2)} \quad (13)$$

where $\text{mmse}(\rho)$ is the MMSE in estimating the input from the output of a Gaussian channel as a function of the SNR ρ . For PPM, we have the following result

Theorem 4.1: The MMSE for PPM on the AWGN channel with SNR ρ is

$$\text{mmse}(\rho) = 1 - \mathbb{E} \left[\frac{e^{2\sqrt{\rho}(\sqrt{\rho} + Z_1)} + (Q-1)e^{2\sqrt{\rho}Z_2}}{\left(e^{\rho + \sqrt{\rho}Z_1} + \sum_{k=2}^Q e^{\sqrt{\rho}Z_k} \right)^2} \right], \quad (14)$$

where $Z_i \sim \mathcal{N}(0, 1)$ for $i = 1, \dots, Q$.

Proof: See Appendix I. ■

Note that both (12) and (14) can be evaluated using standard Monte-Carlo methods.

V. OUTAGE PROBABILITY ANALYSIS WITH CSIR

For the CSIR case, we employ uniform power allocation, i.e. $p_1 = \dots = p_B = \text{snr}$. For codewords transmitted over B blocks, obtaining a closed form analytic expression for the outage probability is intractable. Even for $B = 1$, in some cases, for example the lognormal and gamma-gamma distributions, determining the exact distribution of H can be a difficult task. Instead, as

³The $\log(2)$ term arises because we have defined $I^{\text{awgn}}(\rho)$ in bits/channel usage.

we shall see, obtaining the asymptotic behaviour of the outage probability is substantially simpler. Towards this end, and following the footsteps of [20, 40], we derive the *SNR exponent*.

Theorem 5.1: The outage SNR exponents for a MIMO FSO communications system modeled by (2) are given as follows:

$$d_{(\log \text{snr})^2}^{\text{ln}} = \frac{MN}{8 \log(1 + \sigma_I^2)} (1 + \lfloor B(1 - R_c) \rfloor) \quad (15)$$

$$d_{(\log \text{snr})}^{\text{exp}} = \frac{MN}{2} (1 + \lfloor B(1 - R_c) \rfloor), \quad (16)$$

$$d_{(\log \text{snr})}^{\text{gg}} = \frac{MN}{2} \min(\alpha, \beta) (1 + \lfloor B(1 - R_c) \rfloor), \quad (17)$$

for lognormal, exponential, and gamma-gamma cases respectively, where $R_c = R/\log_2(Q)$ is the rate of the binary code and

$$d_{(\log \text{snr})^k} \triangleq - \lim_{\text{snr} \rightarrow \infty} \frac{\log P_{\text{out}}(\text{snr}, R)}{(\log \text{snr})^k} \quad k = 1, 2. \quad (18)$$

Proof: See Appendix II. ■

Proposition 5.1: The outage SNR exponents given in Theorem 5.1, are achievable by random coding over PPM constellations whenever $B(1 - R_c)$ is not an integer.

Proof: The proof follows from the proof of Theorem 5.1 and the proof of [20, Th. 1]. ■

The above proposition implies that the outage exponents given in Theorem 5.1 are the optimal SNR exponents over the channel, i.e. the outage probability is a lower bound to the error probability of any coding scheme, its corresponding exponents (given in Theorem 5.1) are an upper bound to the exponent of coding schemes. From Proposition 5.1, we can achieve the outage exponents with a particular coding scheme (random coding, in this case), and therefore, the exponents in Theorem 5.1 are optimal.

From (15)-(17) we immediately see the benefits of spatial and block diversity on the system. In particular, each exponent is proportional to: the number of lasers times the number of apertures, reflecting the spatial diversity; a channel related parameter that is dependent on the scintillation distribution; and the Singleton bound, which is the optimal rate-diversity tradeoff for Rayleigh-faded block fading channels [18–20].

Comparing the channel related parameters in (15)-(17) the effects of the scintillation distribution on the outage probability are directly visible. For the lognormal case, the channel related parameter is $8 \log(1 + \sigma_I^2)$ and hence is directly linked to the SI. Moreover, for small $\sigma_I^2 < 1$,

$8 \log(1 + \sigma_I^2) \approx 8\sigma_I^2$ and the SNR exponent is inversely proportional to the SI. For the exponential case, the channel related parameter is a constant $1/2$ as expected, since the SI is constant. For the gamma-gamma case the channel related parameter is $\min(\alpha, \beta)/2$, which highlights an interesting connection between the outage probability and recent results in the theory of optical scintillation. For gamma-gamma distributed scintillation, the fading coefficient results from the product of two independent random variables, i.e. $\tilde{H} = XY$, where X and Y model fluctuations due to large scale and small scale cells. Large scale cells cause refractive effects that mainly distort the wave front of the propagating beam, and tend to steer the beam in a slightly different direction (i.e. beam wander). Small scale cells cause scattering by diffraction and therefore distort the amplitude of the wave through beam spreading and irradiance fluctuations [4, p. 160]. The parameters α, β are related to the large and small scale fluctuation variances via $\alpha = \sigma_X^{-2}$ and $\beta = \sigma_Y^{-2}$. For a plane wave (neglecting inner/outer scale effects) $\sigma_Y^2 > \sigma_X^2$, and as the strength of the optical turbulence increases, the small scale fluctuations dominate and $\sigma_Y^2 \rightarrow 1$ [4, p. 336]. This implies that the SNR exponent is exclusively dependent on the small scale fluctuations. Moreover, in the strong fluctuation regime, $\sigma_Y^2 \rightarrow 1$, the gamma-gamma distribution reduces to a K-distribution [4, p. 368], and the system has the same SNR exponent as the exponential case typically used to model very strong fluctuation regimes.

In comparing the lognormal exponent with the other cases, we observe a striking difference. For the lognormal case (15) implies the outage probability is dominated by a $(\log(\text{snr}))^2$ term, whereas for exponential and gamma-gamma scintillation it is dominated by a $\log(\text{snr})$ term. Thus the outage probability decays much more rapidly with SNR for the lognormal case than it does for the exponential or gamma-gamma cases. Furthermore, for the lognormal case, the slope of the outage probability curve, when plotted on a log-log scale, will not converge to a constant value. In fact, a constant slope curve will only be observed when plotting the outage probability on a $\log\text{-(}\log\text{)}^2$ scale.

In deriving (15) (see Appendix II-A) we do not rely on the lognormal approximation⁴, which has been used on a number occasions in the analysis of FSO MIMO channels, e.g. [5, 12, 29]. Under this approximation, H is lognormal distributed (7) with parameters $\mu = -\log(1 +$

⁴This refers to approximating the distribution of the sum of lognormal distributed random variables as lognormal [41–44].

$\sigma_I^2/(MN)$) and $\sigma^2 = -\mu$, and we obtain the approximated exponent

$$d_{(\log \text{snr})^2} \approx \frac{1}{8 \log(1 + \frac{\sigma_I^2}{MN})} (1 + \lfloor B(1 - R_c) \rfloor). \quad (19)$$

Comparing (15) and (19) we see that although the lognormal approximation also exhibits a $(\log(\text{snr}))^2$ term, it has a different slope than the true SNR exponent. The difference is due to the approximated and true pdfs having different behaviours in the limit as $h \rightarrow 0$. However, for very small $\sigma_I^2 < 1$, using $\log(1 + x) \approx x$ (for $x < 1$) in (15) and (19) we see that they are approximately equal.

For the special case of single block transmission, $B = 1$, it is straightforward to express the outage probability in terms of the cumulative distribution function (cdf) of the scintillation random variable, i.e.

$$P_{\text{out}}(\text{snr}, R) = F_H \left(\sqrt{\frac{\text{snr}_R^{\text{awgn}}}{\text{snr}}} \right) \quad (20)$$

where $F_H(h)$ denotes the cdf of H , and $\text{snr}_R^{\text{awgn}} \triangleq I^{\text{awgn}, -1}(R)$ denotes the SNR value at which the mutual information is equal to R . Table I reports these values for $Q = 2, 4, 8, 16$ and $R = R_c \log_2 Q$, with $R_c = \frac{1}{4}, \frac{1}{2}, \frac{3}{4}$. Therefore, for $B = 1$, we can compute the outage probability analytically when the distribution of H is available, i.e., in the exponential case for $M, N \geq 1$ or in the lognormal and gamma-gamma cases for $M, N = 1$. In the case of exponential scintillation we have that

$$P_{\text{out}}(\text{snr}, R) = \bar{\Gamma} \left(MN, \left(MN(1 + MN) \frac{\text{snr}_R^{\text{awgn}}}{\text{snr}} \right)^{\frac{1}{2}} \right), \quad (21)$$

where $\bar{\Gamma}(a, x) \triangleq \frac{1}{\Gamma(a)} \int_0^x t^{a-1} \exp(-t) dt$ denotes the regularised (lower) incomplete gamma function [36, p.260]. For the lognormal and gamma-gamma scintillation with $MN > 1$, we must resort to numerical methods. This involved applying the fast Fourier transform (FFT) to $f_{\bar{H}}$ to numerically compute its characteristic function, taking it to the MN th power, and then applying the inverse FFT to obtain f_H . This method yields very accurate numerical computations of the outage probability in only a few seconds.

Outage probability curves for the $B = 1$ case are shown on the left in Fig. 2. For the lognormal case, we see that the curves do not have constant slope for large SNR, while, for the exponential and gamma-gamma cases, a constant slope is clearly visible. We also see the benefits of MIMO, particularly in the exponential and gamma-gamma cases, where the SNR exponent has increased from $1/2$ and 1 to 2 and 4 respectively.

VI. OUTAGE PROBABILITY ANALYSIS WITH CSIT

In this section we consider the case where the transmitter and receiver both have perfect CSI knowledge. In this case, the transmitter determines the optimal power allocation that minimises the outage probability for a fixed rate, subject to a power constraint [21]. The results of this section are based on the application of results from [22] to PPM and the scintillation distributions of interest. Using these results we uncover new insight as to how key design parameters influence the performance of the system. Moreover, we show that large power savings are possible compared to the CSIR case.

For the short-term power constraint given by (4), the optimal power allocation is given by mercury-waterfilling at each channel realisation [22, 45],

$$p_b = \frac{1}{h_b^2} \text{mmse}^{-1} \left(\min \left\{ \frac{Q-1}{Q}, \frac{\eta}{h_b^2} \right\} \right), \quad (22)$$

for $b = 1, \dots, B$ where $\text{mmse}^{-1}(u)$ is the inverse-MMSE function and η is chosen to satisfy the power constraint.⁵ From [22, Prop. 1] it is apparent that the SNR exponent for the CSIT case under short-term power constraints is the same as the CSIR case.

For the long-term power constraint given by (5) the optimal power allocation is [22]

$$\mathbf{p} = \begin{cases} \wp, & \sum_{b=1}^B \wp_b \leq s \\ \mathbf{0}, & \text{otherwise,} \end{cases} \quad (23)$$

where

$$\wp_b = \frac{1}{h_b^2} \text{mmse}^{-1} \left(\min \left\{ \frac{Q-1}{Q}, \frac{1}{\eta h_b^2} \right\} \right), \quad b = 1, \dots, B \quad (24)$$

and s is a threshold such that $s = \infty$ if $\lim_{s \rightarrow \infty} \mathbb{E}_{\mathcal{R}(s)} \left[\frac{1}{B} \sum_{b=1}^B \wp_b \right] \leq P$, and

$$\mathcal{R}(s) \triangleq \left\{ \mathbf{h} \in \mathbb{R}_+^B : \frac{1}{B} \sum_{b=1}^B \wp_b \leq s \right\}, \quad (25)$$

otherwise, s is chosen such that $P = \mathbb{E}_{\mathcal{R}(s)} \left[\frac{1}{B} \sum_{b=1}^B \wp_b \right]$. In (24), η is now chosen to satisfy the rate constraint

$$\frac{1}{B} \sum_{b=1}^B I^{\text{awgn}} \left(\text{mmse}^{-1} \left(\min \left\{ \frac{Q-1}{Q}, \frac{1}{\eta h_b^2} \right\} \right) \right) = R \quad (26)$$

⁵Note that in [22, 45], the minimum in (22) is between 1 and $\frac{\eta}{h_b^2}$. For QPPM, $\text{mmse}(0) = \frac{Q-1}{Q}$ (see (14)). Hence we must replace 1 with $\frac{Q-1}{Q}$.

From [22], the long-term SNR exponent is given by

$$d_{(\log \text{snr})}^{\text{lt}} = \begin{cases} \frac{d_{(\log \text{snr})}^{\text{st}}}{1 - d_{(\log \text{snr})}^{\text{st}}} & d_{(\log \text{snr})}^{\text{st}} < 1 \\ \infty & d_{(\log \text{snr})}^{\text{st}} > 1 \end{cases}, \quad (27)$$

where $d_{(\log \text{snr})}^{\text{st}}$ is the short-term SNR exponent, i.e., the SNR exponents (15)-(17). Note that $d_{(\log \text{snr})}^{\text{lt}} = \infty$ implies the outage probability curve is vertical, i.e. the power allocation scheme (23) is able to maintain constant instantaneous mutual information (11). The maximum achievable rate at which this occurs is defined as the *delay-limited capacity* [23]. From (27) and (15)-(17), we therefore have the following corollary.

Corollary 6.1: The delay-limited capacity of the channel described by (2) with CSIT subject to long-term power constraint (5) is zero whenever

$$MN \leq \begin{cases} 2(1 + \lfloor B(1 - R_c) \rfloor)^{-1} & \text{exponential} \\ \frac{2}{\min(\alpha, \beta)}(1 + \lfloor B(1 - R_c) \rfloor)^{-1} & \text{gamma-gamma} \end{cases}. \quad (28)$$

For lognormal scintillation, delay-limited capacity is always nonzero.

Corollary 6.1 outlines fundamental design criteria for nonzero delay-limited capacity in FSO communications. Single block transmission ($B = 1$) is of particular importance given the slow time-vary nature of scintillation. From (28), to obtain nonzero delay-limited capacity with $B = 1$, one requires $MN > 2$ and $MN > 2/\min(\alpha, \beta)$ for exponential and gamma-gamma cases respectively. Note that typically, $\alpha, \beta \geq 1$. Thus a 3×1 , 1×3 or 2×2 MIMO system is sufficient for most cases of interest.

In addition, for the special case $B = 1$, the solution (24) can be determined explicitly since

$$\eta = (h^2 \text{mmse}(I^{\text{awgn}, -1}(R)))^{-1} = (h^2 \text{mmse}(\text{snr}_R^{\text{awgn}}))^{-1}. \quad (29)$$

Therefore,

$$\wp^{\text{opt}} = \frac{\text{snr}_R^{\text{awgn}}}{h^2}. \quad (30)$$

Intuitively, (30) implies that for single block transmission, whenever $\text{snr}_R^{\text{awgn}}/h^2 \leq s$, one simply transmits at the minimum power necessary so that the received instantaneous SNR is equal to the SNR threshold ($\text{snr}_R^{\text{awgn}}$) of the code. Otherwise, transmission is turned off. Thus an outage occurs whenever $h < \sqrt{\frac{\text{snr}_R^{\text{awgn}}}{s}}$ and hence

$$P_{\text{out}}(\text{snr}, R) = F_H \left(\sqrt{\frac{\text{snr}_R^{\text{awgn}}}{\gamma^{-1}(\text{snr})}} \right) \quad (31)$$

where $\gamma^{-1}(\text{snr})$ is the solution to the equation $\gamma(s) = \text{snr}$, i.e.,

$$\gamma(s) \triangleq \text{snr}_R^{\text{awgn}} \int_{\nu}^{\infty} \frac{f_H(h)}{h^2} dh, \quad (32)$$

where $\nu \triangleq \sqrt{\frac{\text{snr}_R^{\text{awgn}}}{s}}$. Moreover, the snr at which $P_{\text{out}}(R, \text{snr}) \rightarrow 0$ is precisely $\lim_{s \rightarrow \infty} \gamma(s)$. In other words, the minimum long-term average SNR required to maintain a constant mutual information of R bits per channel use, denoted by $\overline{\text{snr}}$, is

$$\overline{\text{snr}}_R^{\text{awgn}} = \text{snr}_R^{\text{awgn}} \int_0^{\infty} \frac{f_H(h)}{h^2} dh. \quad (33)$$

Hence, recalling that $\text{snr}_R^{\text{awgn}} = I^{\text{awgn}, -1}(R)$, the delay-limited capacity (under the constraint of PPM) is⁶

$$C_d(\text{snr}) = I^{\text{awgn}} \left(\frac{\text{snr}}{\int_0^{\infty} \frac{f_H(h)}{h^2} dh} \right). \quad (34)$$

In the cases where the distribution of H is known in closed form, (32) can be solved explicitly, hence yielding the exact expressions for outage probability (31) and delay-limited capacity (34). For lognormal distributed scintillation with $B = M = N = 1$, we have that

$$\gamma^{\text{ln}}(s) = \frac{1}{2} \text{snr}_R^{\text{awgn}} (1 + \sigma_I^2)^4 \text{erfc} \left(\frac{3 \log(1 + \sigma_I^2) + \frac{1}{2} \log \text{snr}_R^{\text{awgn}} - \frac{1}{2} \log s}{\sqrt{2 \log(1 + \sigma_I^2)}} \right), \quad (35)$$

and

$$C_d^{\text{ln}}(\text{snr}) = I^{\text{awgn}} \left(\frac{\text{snr}}{(1 + \sigma_I^2)^4} \right), \quad (36)$$

where we have explicitly solved the integrals in (32) and (34) respectively.

For the exponential case with $B = 1$, we obtain,

$$\gamma^{\text{exp}}(s) = \text{snr}_R^{\text{awgn}} \frac{MN(1 + MN)}{(MN - 1)(MN - 2)} \bar{\Gamma} \left(MN - 2, \sqrt{MN(1 + MN)} \frac{\text{snr}_R^{\text{awgn}}}{s} \right), \quad (37)$$

and

$$C_d^{\text{exp}}(\text{snr}) = \begin{cases} I^{\text{awgn}} \left(\frac{(MN-1)(MN-2)}{MN(1+MN)} \text{snr} \right) & MN > 2 \\ 0 & \text{otherwise.} \end{cases} \quad (38)$$

⁶Note that a similar expression was derived in [23].

For the gamma-gamma case with $B = M = N = 1$, $\gamma^{\text{gg}}(s)$ can be expressed in terms of hypergeometric functions, which are omitted for space reasons. The delay-limited capacity, however, reduces to a simpler expression⁷

$$C_d^{\text{gg}}(\text{snr}) = \begin{cases} I_{\text{awgn}} \left(\frac{(\alpha-2)(\alpha-1)(\beta-2)(\beta-1)}{(\alpha\beta)(\alpha+1)(\beta+1)} \text{snr} \right) & \alpha, \beta > 2 \\ 0 & \text{otherwise.} \end{cases} \quad (39)$$

Fig. 2 (right) compares the outage probability for the $B = 1$ CSIT case (with long-term power constraints) for each of the scintillation distributions. For $MN = 1$ we see that the outage curve is vertical only for the lognormal case, since $C_d = 0$ for the exponential and gamma-gamma cases. In these cases one must code over multiple blocks for $C_d > 0$, i.e. from Corollary 6.1, $B \geq 6$ and $B \geq 4$ for the exponential and gamma-gamma cases respectively (with $R_c = 1/2$). Comparing the CSIR and CSIT cases in Fig. 2 we can see that very large power savings are possible when CSI is known at the transmitter. These savings are further illustrated in Table II, which compares the SNR required to achieve $P_{\text{out}} < 10^{-5}$ (denoted by snr^*) for the CSIR case, and the long-term average SNR required for $P_{\text{out}} \rightarrow 0$ in the CSIT case (denoted by $\overline{\text{snr}}$, which is given by (33)). Note that in the CSIT case, the values of $\overline{\text{snr}}$ given in the parentheses' is the minimum SNR required to achieve $P_{\text{out}} < 10^{-5}$, since $C_d = 0$ for these cases (i.e. $\overline{\text{snr}} = \infty$). From Table II we see that the power saving is at least around 15 dB, and in some cases as high as 50 dB. We also see the combined benefits of MIMO and power control, e.g. at $MN = 4$, the system is only 3.7 dB (lognormal) to 5.2 dB (exponential) from the capacity of nonfading PPM channel ($\text{snr}_{1/2}^{\text{awgn}} = 3.18$ dB).

VII. CONCLUSION

In this paper we have analysed the outage probability of the MIMO Gaussian FSO channel under the assumption of PPM and non-ideal photodetection, for lognormal, exponential and gamma-gamma distributed scintillation. When CSI is known only at the receiver, we have shown that the SNR exponent is proportional to the number lasers and apertures, times a channel related parameter (dependent on the scintillation distribution), times the Singleton bound, even in the cases where a closed form expression of the equivalent SISO channel distribution is not available

⁷Note that since we assume the normalisation $\mathbb{E}[H^2] = 1$, then $\int_0^\infty \frac{f_H(h)}{h^2} dh = \frac{1}{c^2} \int_0^\infty \frac{f_{\tilde{H}}(u)}{u^2} du$, where $c = 1/\sqrt{1 + \sigma_I^2}$ and $f_{\tilde{H}}(h)$ is defined as in (9) such that $\mathbb{E}[\tilde{H}] = 1$.

in closed-form. When the scintillation is lognormal distributed, we have shown that the outage probability is dominated by a $(\log(\text{snr}))^2$ term, whereas for the exponential and gamma-gamma cases it is dominated by a $\log(\text{snr})$ term. When CSI is also known at the transmitter, we applied the power control techniques of [22] to PPM to show that very significant power savings are possible.

APPENDIX I

PROOF OF THEOREM 4.1

Suppose PPM symbols are transmitted over an AWGN channel, the non-fading equivalent of (2). The received noisy symbols are given by $\mathbf{y} = \sqrt{\rho}\mathbf{x} + \mathbf{z}$, where $\mathbf{x} \in \mathcal{X}^{\text{ppm}}$ (we have dropped the time index ℓ for brevity of notation).

Using Bayes' rule [46], the MMSE estimate is

$$\hat{\mathbf{x}} = \mathbb{E}[\mathbf{x}|\mathbf{y}] = \sum_{q=1}^Q \frac{\mathbf{e}_q \exp(\sqrt{\rho}y_q)}{\sum_{k=1}^Q \exp(\sqrt{\rho}y_k)}. \quad (40)$$

From (40) the i th element of $\hat{\mathbf{x}}$ is

$$\hat{x}_i = \frac{\exp(\sqrt{\rho}y_i)}{\sum_{k=1}^Q \exp(\sqrt{\rho}y_k)}. \quad (41)$$

Using the orthogonality principle [47] $\text{mmse}(\rho) = \mathbb{E}[\|\mathbf{x} - \hat{\mathbf{x}}\|^2] = \mathbb{E}[\|\mathbf{x}\|^2] - \mathbb{E}[\|\hat{\mathbf{x}}\|^2]$. Since $\|\mathbf{e}_q\|^2 = 1$ for all $q = 1, \dots, Q$, then $\mathbb{E}[\|\mathbf{x}\|^2] = 1$. Due to the symmetry of QPPM we need only consider the case when $\mathbf{x} = \mathbf{e}_1$ was transmitted. Hence,

$$\text{mmse}(\rho) = 1 - (\mathbb{E}[\hat{x}_1^2] + (Q-1)\mathbb{E}[\hat{x}_2^2]). \quad (42)$$

Now $y_1 = \sqrt{\rho} + z_1$ and $y_i = z_i$ for $i = 2, \dots, Q$, where z_q is a realisation of a random variable $Z_q \sim \mathcal{N}(0, 1)$ for $q = 1, \dots, Q$. Hence, substituting these values in (41) and taking the expectation (42) yields the result given the theorem.

APPENDIX II

PROOF OF THEOREM 5.1

We begin by defining a normalised (with respect to SNR) fading coefficient, $\zeta_b^{m,n} = -\frac{2 \log \bar{h}_b^{m,n}}{\log \text{snr}}$, which has a pdf

$$f_{\zeta_b^{m,n}}(\zeta) = \frac{\log \text{snr}}{2} e^{-\frac{1}{2}\zeta \log \text{snr}} f_{\bar{H}}\left(e^{-\frac{1}{2}\zeta \log \text{snr}}\right). \quad (43)$$

Since we are only concerned with the asymptotic outage behaviour, the scaling of the coefficients is irrelevant, and to simplify our analysis we assume $\mathbb{E}[\hat{H}^2] = 1$. Hence the instantaneous SNR for block b is given by

$$\rho_b = \text{snr} h_b^2 = \left(\frac{1}{MN} \sum_{m=1}^M \sum_{n=1}^N \text{snr}^{\frac{1}{2}(1-\zeta_b^{m,n})} \right)^2 \quad (44)$$

for $b = 1, \dots, B$. Therefore,

$$\begin{aligned} \lim_{\text{snr} \rightarrow \infty} I^{\text{awgn}}(\rho_b) &= \begin{cases} 0 & \text{if all } \zeta_b^{m,n} > 1 \\ \log_2 Q & \text{at least one } \zeta_b^{m,n} < 1 \end{cases} \\ &= \log_2 Q (1 - \mathbf{1}\{\zeta_b \succ \mathbf{1}\}) \end{aligned}$$

where $\zeta_b \triangleq (\zeta_b^{1,1}, \dots, \zeta_b^{M,N})$, $\mathbf{1}\{\cdot\}$ denotes the indicator function, $\mathbf{1} \triangleq (1, \dots, 1)$ is a $1 \times MN$ vector of 1's, and the notation $\mathbf{a} \succ \mathbf{b}$ for vectors $\mathbf{a}, \mathbf{b} \in \mathbb{R}^k$ means that $a_i > b_i$ for $i = 1, \dots, k$.

From the definition of outage probability (10), we have

$$P_{\text{out}}(\text{snr}, R) = \Pr(I_h(\text{snr}) < R) = \int_{\mathcal{A}} f(\zeta) d\zeta \quad (45)$$

where $\zeta \triangleq (\zeta_1, \dots, \zeta_B)$ is a $1 \times BMN$ vector of normalised fading coefficients, $f(\zeta)$ denotes their joint pdf, and

$$\mathcal{A} = \left\{ \zeta \in \mathbb{R}^{BMN} : \sum_{b=1}^B \mathbf{1}\{\zeta_b \succ \mathbf{1}\} > B(1 - R_c) \right\} \quad (46)$$

is the asymptotic outage set. We now compute the asymptotic behaviour of the outage probability, i.e.

$$- \lim_{\text{snr} \rightarrow \infty} \log P_{\text{out}}(\text{snr}, R) = - \lim_{\text{snr} \rightarrow \infty} \log \int_{\mathcal{A}} f(\zeta) d\zeta. \quad (47)$$

A. Lognormal case

From (7) and (43) we obtain the joint pdf,

$$f(\zeta) \doteq \exp \left(- \frac{(\log \text{snr})^2}{8\sigma^2} \sum_{b=1}^B \sum_{m=1}^M \sum_{n=1}^N (\zeta_b^{m,n})^2 \right), \quad (48)$$

where we have ignored terms of order less than $(\log \text{snr})^2$ in the exponent and constant terms independent of ζ in front of the exponential. Combining (47), (48), and using Varadhan's lemma [48],

$$- \lim_{\text{snr} \rightarrow \infty} \log P_{\text{out}}(\text{snr}, R) = \frac{(\log \text{snr})^2}{8\sigma^2} \inf_{\mathcal{A}} \left\{ \sum_{b=1}^B \sum_{m=1}^M \sum_{n=1}^N (\zeta_b^{m,n})^2 \right\}$$

The above infimum occurs when any κ of the ζ_b vectors are such that $\zeta_b \succ 1$ and the other $B - \kappa$ vectors are zero, where κ is a unique integer satisfying

$$\kappa < B(1 - R_c) \leq \kappa + 1. \quad (49)$$

Hence, it follows that $\kappa = 1 + \lfloor B(1 - R_c) \rfloor$ and thus,

$$-\lim_{\text{snr} \rightarrow \infty} \log P_{\text{out}}(\text{snr}, R) = \frac{(\log \text{snr})^2}{8\sigma^2} MN (1 + \lfloor B(1 - R_c) \rfloor). \quad (50)$$

Dividing both sides of (50) by $(\log \text{snr})^2$ the SNR exponent (15) is obtained.

B. Exponential case

From (8) and (43) we obtain the joint pdf,

$$f(\zeta) \doteq \exp \left(-\log \text{snr} \frac{MN}{2} \sum_{b=1}^B \sum_{m=1}^M \sum_{n=1}^N \zeta_b^{m,n} \right), \quad (51)$$

where we have ignored exponential terms in the exponent and constant terms independent of ζ in front of the exponential.

Following the same steps as the lognormal case i.e. the defining the same asymptotic outage set and application of Varadhan's lemma [48], the SNR exponent (16) is obtained.

C. Gamma-gamma case

Let us first assume $\alpha > \beta$. From (9) and (43) we obtain the joint pdf,

$$f_{\zeta_b^{m,n}}(\zeta) \doteq \exp \left(-\frac{\beta}{2} \zeta \log \text{snr} \right), \quad \zeta > 0 \quad (52)$$

for large snr, where we have used the approximation $K_\nu(x) \approx \frac{1}{2} \Gamma(\nu) (\frac{1}{2}x)^{-\nu}$ for small x and $\nu > 0$ [36, p. 375]. The extra condition, $\zeta > 0$, is required to ensure the argument of the Bessel function approaches zero as $\text{snr} \rightarrow \infty$ to satisfy the requirements of the aforementioned approximation. For the case $\beta > \alpha$ we need only swap α and β in (52). Hence we have the joint pdf

$$f(\zeta) \doteq \exp \left(-\frac{\min(\alpha, \beta) \log \text{snr}}{2} \sum_{b=1}^B \sum_{m=1}^M \sum_{n=1}^N \zeta_b^{m,n} \right), \quad \zeta \succ \mathbf{0}. \quad (53)$$

Now, following the same steps as in the lognormal and exponential cases, with the additional constraint $\zeta_b \succ \mathbf{0}$, the SNR exponent (17) is obtained

REFERENCES

- [1] H. Willebrand and B. S. Ghuman, *Free-Space Optics: Enabling Optical Connectivity in Today's Networks*, Sams Publishing, Indianapolis, USA, 2002.
- [2] J. W. Strohbehm, Ed., *Laser Beam Propagation in the Atmosphere*, vol. 25, Springer-Verlag, Germany, 1978.
- [3] R. M. Gagliardi and S. Karp, *Optical communications*, John Wiley & Sons, Inc., Canada, 1995.
- [4] L. C. Andrews and R. L. Phillips, *Laser Beam Propagation through Random Media*, SPIE Press, USA, 2nd edition, 2005.
- [5] N. Letzepis, I. Holland, and W. Cowley, "The Gaussian free space optical MIMO channel with Q -ary pulse position modulation," *to appear IEEE Trans. Wireless Commun.*, 2008.
- [6] K. Chakraborty, S. Dey, and M. Franceschetti, "On outage capacity of MIMO Poisson fading channels," in *Proc. IEEE Int. Symp. Inform. Theory*, July 2007.
- [7] K. Chakraborty and P. Narayan, "The Poisson fading channel," *IEEE Trans. Inform. Theory*, vol. 53, no. 7, pp. 2349–2364, July 2007.
- [8] N. Cvijetic, S. G. Wilson, and M. Brandt-Pearce, "Receiver optimization in turbulent free-space optical MIMO channels with APDs and Q -ary PPM," *IEEE Photon. Tech. Lett.*, vol. 19, no. 2, pp. 103–105, Jan. 2007.
- [9] I. B. Djordjevic, B. Vasic, and M. A. Neifeld, "Multilevel coding in free-space optical MIMO transmission with q -ary PPM over the atmospheric turbulence channel," *IEEE Photon. Tech. Lett.*, vol. 18, no. 14, pp. 1491–1493, July 2006.
- [10] S. G. Wilson, M. Brandt-Pearce, Q. Cao, and J. H. Leveque, "Free-space optical MIMO transmission with Q -ary PPM," *IEEE Trans. on Commun.*, vol. 53, no. 8, pp. 1402–1412, Aug. 2005.
- [11] K. Chakraborty, "Capacity of the MIMO optical fading channel," in *Proc. IEEE Int. Symp. Inform. Theory*, Adelaide, Sept. 2005, pp. 530–534.
- [12] E. J. Lee and V. W. S. Chan, "Part 1: optical communication over the clear turbulent atmospheric channel using diversity," *J. Select. Areas Commun.*, vol. 22, no. 9, pp. 1896–1906, Nov. 2005.
- [13] S. M. Haas and J. H. Shapiro, "Capacity of wireless optical communications," *IEEE J. Select. Areas Commun.*, vol. 21, no. 8, pp. 1346–1356, Oct. 2003.
- [14] A. A. Farid and S. Hranilovic, "Outage capacity optimization for free-space optical links with pointing errors," *IEEE Trans. Light. Tech.*, vol. 25, no. 7, pp. 1702–1710, July 2007.
- [15] L. H. Ozarow, S. Shamai and A. D. Wyner, "Information theoretic considerations for cellular mobile radio," *IEEE Trans. on Vehicular Tech.*, vol. 43, no. 2, pp. 359–378, May 1994.
- [16] E. Biglieri, J. Proakis and S. Shamai, "Fading channels: information-theoretic and communications aspects," *IEEE Trans. on Inform. Theory*, vol. 44, no. 6, pp. 2619–2692, Oct. 1998.
- [17] M. A. Al-Habash, L. C. Andrews, and R. L. Phillips, "Mathematical model for the irradiance probability density function of a laser beam propagating through turbulent media," *SPIE Opt. Eng.*, vol. 40, no. 8, pp. 1554–1562, 2001.
- [18] R. Knopp and P. Humblet, "On coding for block fading channels," *IEEE Trans. on Inform. Theory*, vol. 46, no. 1, pp. 1643–1646, July 1999.
- [19] E. Malkamaki and H. Leib, "Coded diversity on block-fading channels," *IEEE Trans. on Inform. Theory*, vol. 45, no. 2, pp. 771–781, March 1999.
- [20] A. Guillén i Fàbregas and G. Caire, "Coded modulation in the block-fading channel: Coding theorems and code construction," *IEEE Trans. on Information Theory*, vol. 52, no. 1, pp. 262–271, Jan. 2006.
- [21] G. Caire, G. Taricco and E. Biglieri, "Optimum power control over fading channels," *IEEE Trans. on Inform. Theory*, vol. 45, no. 5, pp. 1468–1489, July 1999.

- [22] K. D. Nguyen, A. Guillén i Fàbregas, and L. K. Rasmussen, “Power allocation for discrete-input delay-limited fading channels,” *submitted to IEEE Trans. Inf. Theory*, <http://arxiv.org/abs/0706.2033>, Jun. 2007.
- [23] S. V. Hanly and D. N. C. Tse, “Multiaccess fading channels. II. delay-limited capacities,” *IEEE Trans. on Inform. Theory*, vol. 44, no. 7, pp. 2816–2831, Nov. 1998.
- [24] S. Dolinar, D. Divsalar, J. Hamkins, and F. Pollara, “Capacity of pulse-position modulation (PPM) on Gaussian and Webb channels,” *JPL TMO Progress Report 42-142*, Aug. 2000, URL: lasers.jpl.nasa.gov/PAPERS/OSA/142h.pdf.
- [25] S. Dolinar, D. Divsalar, J. Hamkins, and F. Pollara, “Capacity of PPM on APD-detected optical channels,” in *21st Cent. Military Commun. Conf. Proc.*, Oct. 2000, vol. 2, pp. 876–880.
- [26] X. Zhu and J. M. Kahn, “Performance bounds for coded free-space optical communications through atmospheric turbulence channels,” *IEEE Trans. on Commun.*, vol. 51, no. 8, pp. 1233–1239, Aug. 2003.
- [27] J. Li and M. Uysal, “Optical wireless communications: system model, capacity and coding,” in *IEEE 58th Vehicular Tech. Conf.*, Oct. 2003, vol. 1, pp. 168–172.
- [28] M. K. Simon and V. A. Vlnrotter, “Alamouti-type space-time coding for free-space optical communication with direct detection,” *IEEE Trans. Wireless Commun.*, , no. 1, pp. 35–39, Jan 2005.
- [29] S. M. Navidpour, M. Uysal, and M. Kavehrad, “BER performance of free-space optical transmission with spatial diversity,” *IEEE Trans. on Wireless Commun.*, vol. 6, no. 8, pp. 2813–2819, August 2007.
- [30] L. C. Andrews, R. L. Phillips, C. Y. Hopen, and M. A. Al-Habash, “Theory of optical scintillation,” *J. Opt. Soc. Am. A*, vol. 16, no. 6, pp. 1417–1429, June 1999.
- [31] R. S. Lawrence and J. W. Strohbehn, “A survey of clean-air propagation effects relevant to optical communications,” *Proc. IEEE*, vol. 58, no. 10, pp. 1523–1545, Oct. 1970.
- [32] J. H. Churnside and S. F. Clifford, “Log-normal Rician probability-density function of optical scintillations in the turbulent atmosphere,” *J. Opt. Soc. Am. A*, vol. 4, no. 10, pp. 1923–1930, Oct. 1987.
- [33] R. J. Hill and R. G. Frehlich, “Probability distribution of irradiance for the onset of strong scintillation,” *J. Opt. Soc. Am. A*, vol. 14, no. 7, pp. 1530–1540, July 1997.
- [34] F. S. Vetelino, C. Young, L. Andrews, and J. Rekolons, “Aperture averaging effects on the probability density of irradiance fluctuations in moderate-to-strong turbulence,” *Applied Optics*, vol. 46, no. 11, pp. 2099–2108, April 2007.
- [35] P. Beckmann, *Probability in Communication Engineering*, Harcourt, Brace and World, New York, 1967.
- [36] M. Abramowitz and I. A. Stegun, *Handbook of Mathematical Functions with Formulas, Graphs and Mathematical Tables*, New York: Dover Press, 1972.
- [37] S. Verdú and T. S. Han, “A general formula for channel capacity,” *IEEE Trans. on Inform. Theory*, vol. 40, no. 4, pp. 1147–1157, Jul. 1994.
- [38] T. M. Cover and J. A. Thomas, *Elements of Information Theory*, Wiley Series in Telecommunications, 1991.
- [39] D. Guo, S. Shamai, and S. Verdú, “Mutual information and minimum mean-square error in Gaussian channels,” *IEEE Trans. Inf. Theory*, vol. 51, no. 4, pp. 1261–1282, Apr. 2005.
- [40] L. Zheng and D. Tse, “Diversity and multiplexing: A fundamental tradeoff in multiple antenna channels,” *IEEE Trans. on Inform. Theory*, vol. 49, no. 5, May 2003.
- [41] R. L. Mitchell, “Permanence of the log-normal distribution,” *J. Opt. Soc. Am.*, 1968.
- [42] S. B. Slimane, “Bounds on the distribution of a sum of independent lognormal random variables,” *IEEE Trans. on Commun.*, vol. 49, no. 6, pp. 975–978, June 2001.

- [43] N. C. Beaulieu and X. Qiong, “An optimal lognormal approximation to lognormal sum distributions,” *IEEE Trans. Vehic. Tech.*, vol. 53, no. 2, March 2004.
- [44] N. C. Beaulieu and F. Rajwani, “Highly accurate simple closed-form approximations to lognormal sum distributions and densities,” *IEEE Commun. Let.*, vol. 8, no. 12, pp. 709–711, Dec. 2004.
- [45] A. Lozano, A. M. Tulino, and S. Verdú, “Optimum power allocation for parallel Gaussian channels with arbitrary input distributions,” *IEEE Trans. Inform. Theory*, vol. 52, no. 7, pp. 3033–3051, July 2006.
- [46] A. Papoulis, *Probability, random variables, and stochastic processes*, McGraw-Hill, 1991.
- [47] S. M. Kay, *Fundamentals of Statistical Signal Processing: Estimation Theory*, Prentice Hall Int. Inc., USA, 1993.
- [48] A. Dembo and O. Zeitouni, *Large Deviations Techniques and Applications*, Number 38 in Applications of Mathematics. Springer Verlag, 2nd edition, April 1998.

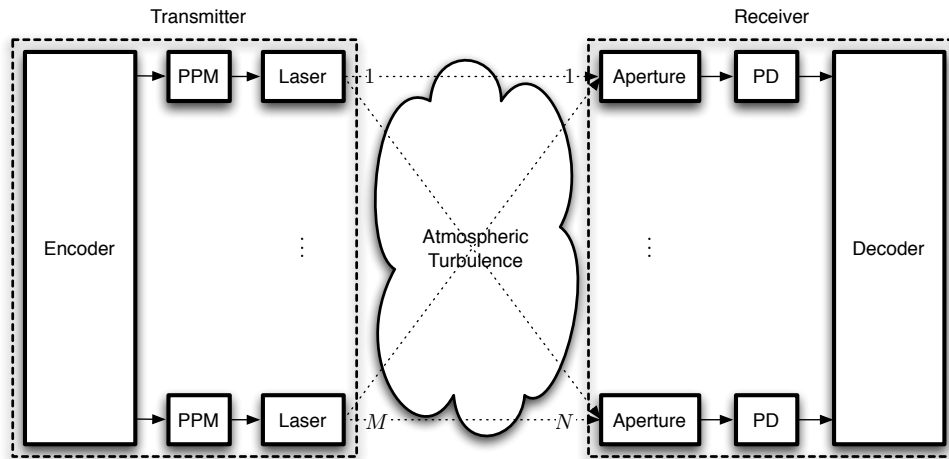


Fig. 1. Block diagram of an $M \times N$ MIMO FSO system.

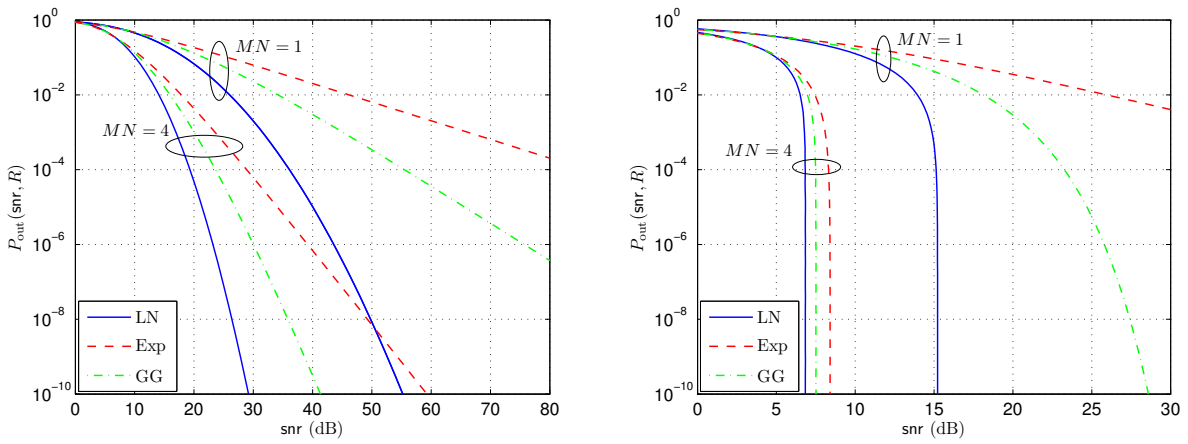


Fig. 2. Outage probability curves for the CSIR (left) and CSIT (right) cases with $\sigma_I^2 = 1$, $B = 1$, $Q = 2$, $R_c = 1/2$, $\text{snr}_{1/2}^{\text{awgn}} = 3.18$ dB: lognormal (solid); exponential (dashed); and, gamma-gamma distributed scintillation (dot-dashed), $\alpha = 2$, $\beta = 3$.

TABLE I
 MINIMUM SIGNAL-TO-NOISE RATIO $\text{snr}_R^{\text{awgn}}$ (IN DECIBELS) FOR RELIABLE COMMUNICATION FOR TARGET RATE
 $R = R_c \log_2 Q$.

Q	$R_c = \frac{1}{4}$	$R_c = \frac{1}{2}$	$R_c = \frac{3}{4}$
2	-0.7992	3.1821	6.4109
4	0.2169	4.0598	7.0773
8	1.1579	4.8382	7.7222
16	1.9881	5.5401	8.3107

TABLE II
 COMPARISON OF CSIR AND CSIT CASES WITH $B = 1$, $R = 1/2$, $Q = 2$, $\sigma_I^2 = 1$, $\alpha = 2$, $\beta = 3$. BOTH snr^* AND $\overline{\text{snr}}$ ARE MEASURED IN DECIBELS.

MN	lognormal		exponential		gamma-gamma	
	snr^*	$\overline{\text{snr}}$	snr^*	$\overline{\text{snr}}$	snr^*	$\overline{\text{snr}}$
1	40.1	15.2	106.2	(56.2)	65.6	(24.5)
2	29.2	9.9	57.9	(17.8)	40.7	12.2
3	24.4	7.9	42.0	11.0	31.7	9.0
4	21.5	6.9	34.1	8.4	26.9	7.5